



ELSEVIER

Nuclear Physics A 633 (1998) 547–562

---

---

NUCLEAR  
PHYSICS A

---

---

## Thermal source parameters in Au+Au central collisions at 35 A MeV

P. Désesquelles<sup>a</sup>, M. D'Agostino<sup>b</sup>, A.S. Botvina<sup>b,c</sup>, M. Bruno<sup>b</sup>,  
N. Colonna<sup>d</sup>, A. Ferrero<sup>e,f</sup>, M.L. Fiandri<sup>b</sup>, E. Fuschini<sup>b</sup>, F. Gramegna<sup>g</sup>,  
I. Iori<sup>e</sup>, G.V. Margagliotti<sup>h</sup>, P.F. Mastinu<sup>i</sup>, P.M. Milazzo<sup>h</sup>, A. Moroni<sup>e</sup>,  
F. Petruzzelli<sup>e</sup>, R. Rui<sup>h</sup>, G. Vannini<sup>h</sup>, J.D. Dinius<sup>j</sup>, C.K. Gelbke<sup>j</sup>,  
T. Glasmacher<sup>j</sup>, D.O. Handzy<sup>j</sup>, W.C. Hsi<sup>j</sup>, M. Huang<sup>j</sup>, M.A. Lisa<sup>j</sup>,  
W.G. Lynch<sup>j</sup>, C.P. Montoya<sup>j</sup>, G.F. Peaslee<sup>j</sup>, L. Phair<sup>j</sup>, C. Schwarz<sup>j</sup>,  
M.B. Tsang<sup>j</sup>, C. Williams<sup>j</sup>

### Multics/Miniball Collaboration

<sup>a</sup> *Institut des Sciences Nucléaires, IN2P3-CNRS et Université Joseph Fourier, Grenoble, France*

<sup>b</sup> *Dipartimento di Fisica and INFN, Bologna, Italy*

<sup>c</sup> *Institute for Nuclear Research, Russian Academy of Science, 117312 Moscow, Russia*

<sup>d</sup> *INFN, Bari, Italy*

<sup>e</sup> *Dipartimento di Fisica and INFN, Milano, Italy*

<sup>f</sup> *C.N.E.A., Buenos Aires, Argentina*

<sup>g</sup> *INFN, Laboratori Nazionali di Legnaro, Italy*

<sup>h</sup> *Dipartimento di Fisica and INFN, Trieste, Italy*

<sup>i</sup> *Dipartimento di Fisica, Padova and INFN, Bologna, Italy*

<sup>j</sup> *National Superconducting Cyclotron Laboratory and Department of Physics and Astronomy, Michigan State University, East Lansing, Michigan 48824, USA*

Received 19 November 1997; revised 9 February 1998; accepted 25 February 1998

---

### Abstract

Central Au+Au collisions at 35 A MeV are analyzed to find the characteristics of a thermal source, in the framework of the statistical multifragmentation model SMM. A recently introduced backtracing protocol provides an effective comparison of theory and experiment. For the first time the *distributions* of the central source parameters (density, mass number, excitation energy) are found. The collective energy of primary fragments is also deduced. It is shown that the backtracing procedure allows an estimation of the pre-equilibrium emission. © 1998 Published by Elsevier Science B.V.

PACS: 24.10.Pa; 25.70.Pq

Keywords: Statistical model; Statistical analysis; Heavy ions; Multifragmentation; Collective flow

---

## 1. Introduction

The multifragment de-excitation of hot compressed composite nuclei formed in central heavy ion collisions at intermediate incident energies, is now a well established process. It has been shown that the time scale for fragment emission is sufficiently short to warrant an investigation based on an instantaneous freeze-out scenario [1–4].

During the pre-equilibrium stage, the hot source (referred to as *composite nucleus* in the following) reaches a maximum compression followed by a rapid expansion, predicted to be self-similar by transport simulations [5,6] for heavy systems like the Au+Au case. How much the entrance channel constraints influence the sharing of excitation energy into the different energetic degrees of freedom (thermal and collective motions) is still a matter of theoretical [1–4,7,8] and experimental investigations [9–13].

There are however theoretical indications [2,8] that a collective energy not exceeding a few  $A$  MeV does not influence the process of fragment formation. Therefore in several experimental papers [9–13] a decoupling has been assumed between the collective energy and the thermal excitation energy.

The commonly used procedure to extract the collective energy from data is to compare the experimental fragment kinetic energies to the thermal+Coulomb emission by a statistically decaying source. The mass and thermal excitation energy or temperature of the source are usually fixed (see Refs. [14]) by requiring the reproduction of the observed charge distribution and/or its low order mean moments (light particle and fragment multiplicities, total detected charge, total charge bound in form of fragments).

The value of the source volume is not constrained by conservation laws, in contrast to other source parameters governed by mass and energy conservation. For each considered reaction/model only a lower and an upper limit on the source volume can be determined by the requirements of non-overlapping fragments and non-zero fragment multiplicity, respectively. This procedure then requires an arbitrary, even if inevitable choice of the freeze-out volume of the emitting system. Due to the correlation between the Coulomb energy and the volume of the source, the value found for the collective energy is thus volume-dependent.

This ambiguity is not eliminated even when performing the comparison of the experimental and predicted kinetic energies for several values of the source volume [15]. As a matter of fact, such a procedure can provide informations on the correlation between volume and flow, but not on the relative probability of different freeze-out volumes.

In this paper a new analysis is reported, performed with the automatic backtracing procedure [16] applied to the experimentally measured Au+Au 35  $A$  MeV central collisions. Working in the framework of a specific model, such a procedure allows to extract the informations contained in the data on the model parameters. In particular the initial distributions of the model parameters which reproduce the global experimental informations can be found.

The reference model used in this analysis is the Copenhagen–Moscow statistical multifragmentation model SMM [2]. This model has already been shown to reproduce the main features of experimental systems close to the present one (see for instance

Refs. [13–15,17]).

The automatic backtracing procedure was already successfully applied to low incident energy central [18] collisions and high incident energy peripheral collisions [19]. In these cases however the analysis was limited to the source mass and excitation energy distributions.

In the present analysis the break-up density, as well as the excitation energy and the mass of the parent nuclei, are treated as event by event free parameters. For the first time, as far as we know, a source break-up density *distribution* is deduced from the data together with the mass and the thermal excitation energy distributions. We shall show that our central collisions are in agreement with a scenario leading to the fragmentation of a very large composite nucleus at a freeze-out density between 1/3 and 1/12 of normal density just above the threshold of the flow development.

## 2. Experiment

The experiment was performed at the National Superconducting Cyclotron Laboratory of the Michigan State University. Beams of Au ions at  $E/A = 35$  A MeV incident energy from the K1200 cyclotron were used to bombard Au foils of approximately  $5 \text{ mg cm}^{-2}$  areal density.

Light charged particles and fragments with charge up to  $Z = 20$  were fully identified by 160 phoswich (fast plastic  $40 \mu\text{m}$  thick + CsI 2 cm thick) detector elements of the MSU *Miniball* [20], covering the angular range from  $23^\circ$  to  $160^\circ$ . The charge identification thresholds were about 2, 3, 4 MeV/nucleon for  $Z = 3, 10, 18$ , respectively.

Fragments with charge up to the beam charge were detected at  $\theta_{\text{lab}}$  from  $3.5^\circ$  to  $23^\circ$  by the *Multics* array [21], with an energy threshold about 1.5 A MeV, nearly independent on fragment charge.

The geometric acceptance of the combined array was greater than 87% of  $4\pi$ . Dynamical calculations [22] indicate that the apparatus is able to detect, with the experimental triggering condition, the generated events up to a maximum impact parameter  $b \approx 11$  fm, even when taking into account energy thresholds,  $Z$ -identification limitations and multiple hits. With these limitations the efficiency (detected charged particle multiplicity/predicted charged particle multiplicity) is calculated to be about  $\sim 80\%$  for impact parameters smaller than 5 fm. Statistical calculations, performed for central collisions with SMM, confirm this value of the efficiency.

The centrality selection has been performed on the basis of the total charged particle multiplicity  $N_c$  [15,23,24]. The reduced impact parameter  $\hat{b}$  for each event was determined as a function of  $N_c$ , assuming that this observable decreases monotonically with impact parameter [25].

The most central 9% of the measured reaction cross section ( $\hat{b} \leq 0.3$ , i.e.  $b \leq 3.5$  fm) was considered in the present analysis. It has been already shown that this event sample corresponds to central collisions leading to the formation of a thermalized composite nucleus [23,24]. Additional constraints on the completeness of the events (detection

of at least 70% of the total charge and total parallel momentum) were here used for a twofold reason. First, completeness reduces the variances induced by the experimental filter of the source parameters we are interested in. Moreover the analyzed observable distributions (e.g. event charge asymmetry and partition) explicitly require a complete detection of the heaviest fragments for each event.

Careful studies were done on the behaviour of the experimental observables as a function of the centrality [26,35]. It was found that  $\hat{b} \leq 0.3$  represents, for this reaction, a limit of the sensitivity of the experimental observables to the centrality of the collisions. Indeed several observables (for instance the fragment multiplicity, the transverse energy and the  $\alpha$ - $\alpha$  azimuthal correlation functions) show very slight changes on their mean values and variances [26], even decreasing  $\hat{b}$  (increasing  $N_c$ ). For  $\hat{b} \leq 0.3$  the  $\cos(\theta_{\text{flow}})$  distribution is flat [24] and observables related to the event shape (sphericity, coplanarity, isotropy ratio) [35] show constant mean values and variances as a function of  $\cos(\theta_{\text{flow}})$ .

These findings are not surprising, since, as shown in Ref. [27] and as found through dynamical calculations [22] performed for our reaction, the observables commonly used for an experimental selection of the impact parameter exhibit large fluctuations around an average value slightly changing for small impact parameters. The capacity of these observables to select very small values of  $b$  is limited and it is almost impossible to give an estimator of  $b$  in these cases.

Since, however, the real difficulty in quantitatively studying fluctuations arises by the superimposition of events with similar but systematically different source parameters (due to the entrance channel geometry) we will verify in the following if different choices of the centrality would change the results of the analysis here presented.

### 3. Automatic backtracing

The protocol used for the comparison of the SMM predictions with the experimental results was introduced in Ref. [16]. The goal of our analysis is to try to reproduce the global experimental informations. To this purpose, we look for the *correlated distributions* of the source variables (vector  $s$  representing the inputs of the SMM code) able to reproduce the experimental correlated distributions of the observable variables (each event is characterized by the vector  $o$  of its observables). This is done using a specific recursive backtracing procedure in the multivariate space of the source and observable variables. We shall deal with three source variables  $s = (A^{c.n.}, E^{c.n.}, V^{c.n.})$ , where  $A^{c.n.}$  is the mass of the source composite nucleus,  $E^{c.n.}$  its excitation energy and  $V^{c.n.}$  the total break up volume.

The experimental data give access to the static (charges of the fragments) and dynamic (velocity vectors) quantities. The latter ones depend on intrinsic as well as collective energy. In order to avoid to give an a-priori hypothesis about the nature of the collective component, only static observables were used in the backtracing procedure (see discussion on Section 6). The SMM model was run with expansion resulting only

from thermal excitation energy and from Coulomb repulsion. This result is used as a reference for the fragment velocities, so that the collective energy is deduced from the difference between the experimental and the simulated fragment kinetic energies.

Furthermore, since only observables concerning the composite nucleus will be analyzed, the pre-equilibrium should not be taken into account. This is realized by considering in the backtracing only fragments with charge larger than four in the experimental sample as well as in the simulated sample. In this way we avoid making any hypothesis on the proportion of the pre-equilibrium light particles among the detected ones.

The whole experimental static information contained in one event can be formalized using the moments of the charge distribution

$$m_i = \sum_{\text{fragments}} z^i, \quad (1)$$

where the sum runs on all fragments including the heaviest one, and the order  $i$  runs from 0 to the maximum experimental multiplicity (twelve in our case). For computational reasons, these moments are standardized (centered and reduced):

$$M_i = (m_i - \langle m_i \rangle) / \sigma(m_i). \quad (2)$$

Finally the observable vector is taken as  $\mathbf{o} : (M_0 \dots M_{12})$ . This is too many variables for the computer capacity since the backtracing procedure entails the handling of a very large matrix representing the model. This matrix ( $P(\mathbf{o}|s)$ , conditional probabilities of the observables for given source variables) contains the correlation between the source and the observable variables. From a computational point of view, the number of elements of this matrix is equal to the product of the number of bins for each source and observable variable. A typical limit, due to the computer memory size, would be seven variables, each one distributed into ten bins ( $10^7$  elements). As we shall deal with three source variables ( $s = (A^{c.n.}, E^{c.n.}, V^{c.n.})$ ) we are left with only four observables to synthesize the maximum experimental information given by the  $m_i$ .

These four observables must be selected in such a way that:

- each one holds a maximum statistical information [28,29];
- two selected variables are not functionally correlated (otherwise, the second one would not add information to the first one);
- they maximize the probability that if they are well reproduced by the backtracing procedure, then observables not directly used in the backtracing procedure are also reproduced.

The optimum variables (called *principal variables*, noted  $p_j$ ) responding to these criteria are given as linear combinations of the primary observables  $M_i$ :

$$p_j = \sum_i \alpha_{ij} M_i, \quad (3)$$

where the sum runs on the observables. The coefficients  $\alpha_{ij}$  can be determined by the so-called Principal Component Analysis (PCA) technique [28,30]. In our case it results that the strongest contributions to the  $p_j$ s (78% of the experimental information)

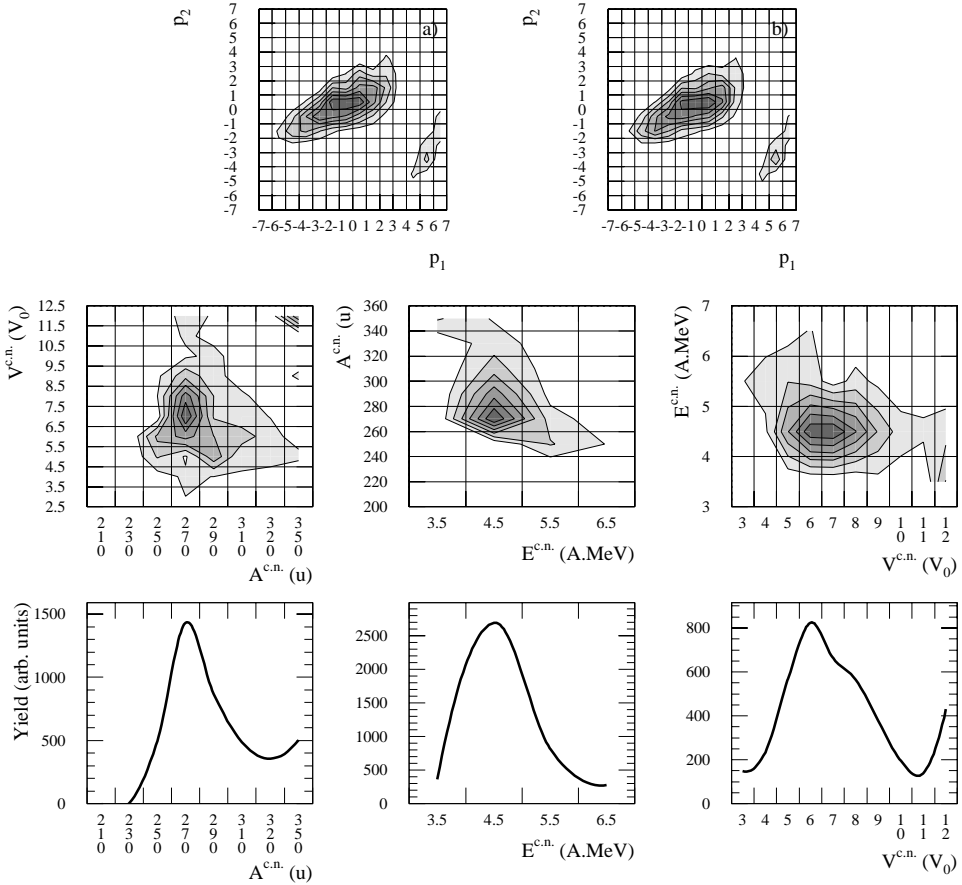


Fig. 1. Event sample seen in the observable (upper row) and source (middle and lower rows) spaces. Upper row: comparison between the correlation of first two principal variables for the experiment (a) and the backtraced SMM (b). Middle row: Two dimensional projections of the correlated distribution of the parameters (source variables) of the SMM code. All the grey scales (7) are linear. Lower row: One dimensional distributions of source variables.

come from the first four charge moments (multiplicity, total charge bound in form of fragments, variance and asymmetry of the charge distribution with respect to the mean value). Higher moments however provide informations on the fluctuations of the events with respect to the mean correlations.

The PCA technique gives us the percentage of the initial information which is retained by considering only a limited number of principal variables. In our case the result is very satisfactory since 98% of the information is retained with only four principal variables. The principal variables are ordered with respect to the information they yield. A large part (83%) of the statistical information is already contained in the  $[p_1, p_2]$  plane, since the first principal variable corresponds to 63% and the second one to 20% of the total information.

The backtracing procedure has converged towards a solution characterized by a low

Kullback–Leibler divergence ( $D = 0.06$ ) [31]. This means that we have a good fit to the experimental four dimensional distribution of the principal variables ( $P^{\text{exp}}(\mathbf{p})$ ). The results in the plane of the two first principal variable [ $p_1, p_2$ ] are shown in Fig. 1 (upper row).

We observe only one large bump in the observable space of Fig. 1, both for the experimental events (a) and for the backtraced ones (b). There is no indication of a mixing of events from different origins or mechanisms. The small ridges on the right part of the plots correspond to events with only two IMFs. The differences among events are only due to the small impact parameter distribution and to physical fluctuations. This result strengthens the claim that all the events in the sample correspond to central collisions inducing the formation of a unique composite nuclear system [15].

#### 4. Source characteristics

The projections of the resulting backtraced distribution of the source variables ( $P(s)$ ) (corrected for the detection efficiency as described in Appendix A of Ref. [16]) on the three planes ( $[V^{\text{c.n.}}, A^{\text{c.n.}}]$ ,  $[A^{\text{c.n.}}, E^{\text{c.n.}}]$ ,  $[E^{\text{c.n.}}, V^{\text{c.n.}}]$ ) are presented in Fig. 1 (middle row). The grid indicates the bins used in the backtracing.  $V_0$  stands for the volume of the source at normal nuclear density. The curves of the lower row of Fig. 1 are the one dimensional distributions of  $A^{\text{c.n.}}$ ,  $E^{\text{c.n.}}$ ,  $V^{\text{c.n.}}$ , respectively.

No structure in the source variable distributions can be seen in our case, contrary to what would be expected when analysing events coming from a large range of impact parameters involving different de-excitation mechanisms [19].

The anticorrelation in the  $[E^{\text{c.n.}}, V^{\text{c.n.}}]$  plane, in agreement with our previous findings [15], is due to the fact that high IMF multiplicity events can be obtained from the model by increasing either the excitation energy or the break up volume.

The mean source characteristics, for the detected events without efficiency corrections, are:  $\langle A^{\text{c.n.}} \rangle = 302$  ( $\sigma_A = 29$ ),  $\langle E^{\text{c.n.}} \rangle = 4.9$  A MeV ( $\sigma_E = 0.6$  A MeV),  $\langle V^{\text{c.n.}} \rangle = 6.2$   $V_0$  ( $\sigma_V = 2.1$   $V_0$ ).

The mean values of the source variables (corrected for the detection efficiency) are:  $\langle A^{\text{c.n.}} \rangle = 287$  ( $\sigma_A = 28$ ),  $\langle E^{\text{c.n.}} \rangle = 4.8$  A MeV ( $\sigma_E = 0.7$  A MeV),  $\langle V^{\text{c.n.}} \rangle = 6.8$   $V_0$  ( $\sigma_V = 1.9$   $V_0$ ). The spurious solution observed in the  $[V^{\text{c.n.}}, A^{\text{c.n.}}]$  plane at the largest considered break-up volume, is due to statistical fluctuations induced by very low local efficiency. After filtering this solution corresponds to a very low number of events. Therefore we have not taken it into account for the calculation of mean values. No important distortion is introduced by the apparatus in  $s$  space.

The composite nucleus size (break-up radius  $R_b \approx 15$  fm) is close to the one of the extra-large source estimated for the same reaction at higher beam energy by Bondorf et al. [14] ( $E_{\text{beam}} = 100$  A MeV,  $R_b = 14$  fm,  $\rho_b = 1/6$   $\rho_0$ ) and by Kämpfer et al. [32] ( $E_{\text{beam}} = 150$  A MeV,  $R_b = 14$  fm).

The mean freeze-out temperature, calculated for the open decay channels through the total energy balance [2], results  $T \approx 5.8$  MeV in almost all the squares of the source

space  $s$ , without correlations with other source parameters. In the framework of *SMM* indeed this composite system breaks-up along the plateau of its caloric curve, with excitation energies above the multifragmentation threshold ( $\sim 3.5$  A MeV for a system of mass  $A_s \approx 300$ ).

## 5. Static observables

Once the source variable distributions are known, a new sample of events can be generated with the simulation code. After taking into account the experimental filter and the selection conditions, the observable distributions obtained from this new sample are the same, within statistical fluctuations, as the ones given by the backtracing procedure (Fig. 1b). Hence one can conclude that the effect of statistical errors (as well of the experimental sample as of the primary simulated sample) are small. From this point of view, the backtraced source distribution can be considered as reliable.

One must also verify that the individual distributions of the “basic” observables which are usually considered to characterize an experimental sample, are also well reproduced. In Fig. 2 we report the comparison between some experimental and predicted static observables: the charge distribution, the fragment ( $Z \geq 4$ ) multiplicity ( $N_{f4}$ ), the total charge bound in form of fragments ( $Z_{b4}$ ), the fourth moment  $m_4$  of the fragment charge distribution.

The same normalization to the total number of events was applied to the experimental and calculated distributions, which thus may be compared on an absolute scale. With this normalization all the vertical axes of Fig. 2 represent the mean multiplicity per event of the considered observable.

A good agreement has also been obtained for all the static observables presented in Ref. [15]. No significant differences are observed even though the simulation distributions do not result from the direct fit to these variables.

Since the main purpose of this work is the study of fragment energies, great care must be paid to the detailed reproduction of the charge partition which strongly affects the Coulomb energy. The good reproduction of the charge distribution and its moments together with the improvement in the description of high charge moments with respect to a calculation with fixed source parameters ( $\langle A^{c.n.} \rangle = 315$ ,  $\langle E^{c.n.} \rangle = 4.8$  A MeV,  $\langle V^{c.n.} \rangle = 6 V_0$ , see Ref. [15]) make us confident that the Coulomb component to fragment energies is better estimated by the backtracing procedure.<sup>1</sup>

The importance of freeze-out volume, treated here as a free parameter, are evident for instance by studying the predicted event charge asymmetry (Fig. 3b) and the event charge partition (Fig. 3c) as a function of freeze-out volume.

<sup>1</sup> In Fig. 2d the fourth moment was calculated excluding the heaviest fragment, in order to not weight too much the slight underestimation by *SMM* at high values of the charge [15].



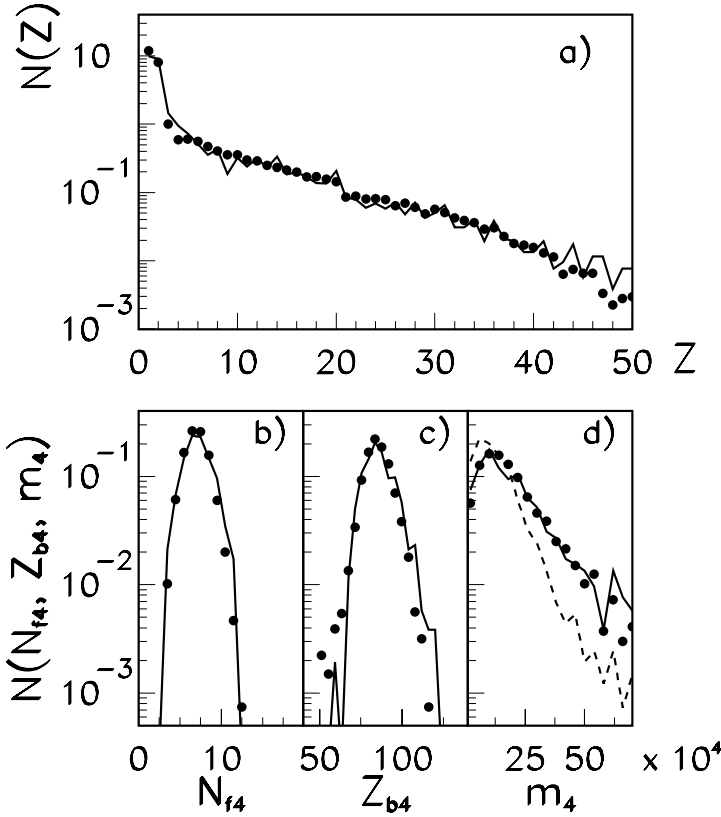


Fig. 2. Comparisons of the observable distributions for the experimental sample (dots) and for the backtracing on SMM (line). Data and predictions were normalized to the total number of events. The vertical axes represent the mean multiplicity per event of the considered observable. (a) Charge distribution, (b) Fragment ( $Z \geq 4$ ) multiplicity ( $N_{f4}$ ), (c) Total charge bound in form of fragments ( $Z_{b4}$ ), (d) Fourth moment  $m_4$  of the fragment charge distribution. The dashed line in panel (d) refers to a SMM calculation with fixed source parameters [15]. The vertical scale of panel (b) applies also to panels (c) and (d).

The charge asymmetry:

$$a_{123} = \frac{\sqrt{(Z_1 - \langle Z \rangle)^2 + (Z_2 - \langle Z \rangle)^2 + (Z_3 - \langle Z \rangle)^2}}{\sqrt{6}\langle Z \rangle}, \tag{4}$$

( $Z_1 \geq Z_2 \geq Z_3$  are the three heaviest fragments in each event and  $\langle Z \rangle$  their mean value) is indeed another static observable very well reproduced by the calculations (Fig. 3a) which can provide informations on charge correlations in each event [33,34].

More asymmetric charge partitions, corresponding to the high tail of the  $Z$ -distribution (e.g. a heavy fragment accompanied by smaller ones) are generated by the model at small freeze-out volumes and the most symmetric ones (small and equal charge fragments, low asymmetry) at larger freeze-out volumes. The Coulomb energy of the heaviest fragments will be higher and that of the lighter fragments will be smaller than the Coulomb energies calculated for a freeze-out volume fixed at its mean value. Therefore

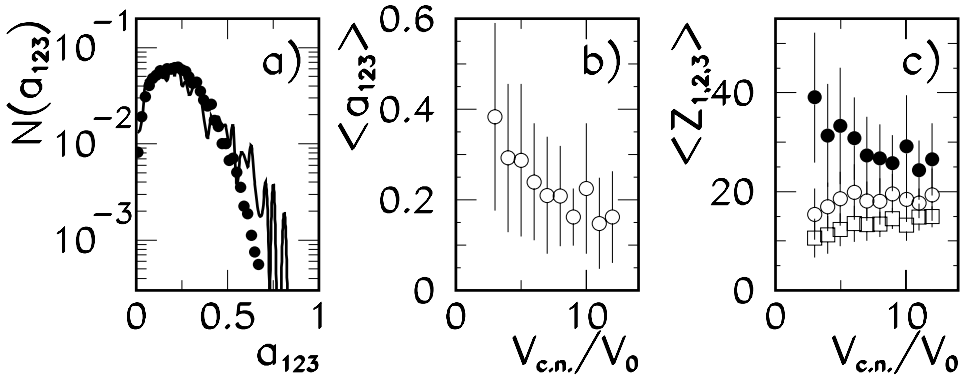


Fig. 3. (a) Experimental (dots) and predicted (line) charge asymmetry distribution (see Eq. (1)). (b) Predicted mean event charge asymmetry as a function of the ratio between the source volume and its normal volume. (c) Predicted mean charges of the three heaviest fragments in each event:  $Z_1$  (dots),  $Z_2$  (open circles),  $Z_3$  (squares) as a function of the ratio between the source volume and its normal volume.

we expect that such modifications will improve the agreement between experimental and predicted dynamical observables [35].

Before going to the comparison of experimental and predicted dynamic observables, we have checked the stability of the source variables going to more central collisions.

Analysing experimental data and predictions for a  $N_c$  range corresponding to impact parameters  $\hat{b} \leq 0.1$ , we found all our results fully confirmed. All the experimental fragment static observables presented in Figs. 2 and 3 do not show any change going to more central collisions and they are well reproduced by calculations. The SMM predicted charge asymmetry and charge partition show the same dependence from the freeze-out volume as in Fig. 3. The variances of all the source characteristics are the same, going to  $\hat{b} \leq 0.1$ . The mean values increase only by few percent. The freeze-out volume increases only by 0.6%, the mean size by about 2% and the thermal excitation energy by about 3%. This gives the indication that the same density (mechanical compression) is seen in the whole range  $\hat{b} \leq 0.3$ . The evolution of the mean source characteristics can be understood in terms of fluctuations of the number of pre-equilibrium particles. Indeed the pre-equilibrium and equilibrium particles have close centre of mass motions and their mean emission velocities are similar.

## 6. Dynamic observables

As mentioned above, the source distribution has been adjusted by the backtracing procedure, in such a way that the experimental static informations are well reproduced. One can now use the corresponding new simulated sample to make a model/experiment comparison of the dynamic variables. We are interested in measuring the amount of collective energy which has possibly to be superimposed to the kinetic energies given by SMM, in order to account for the experimental kinetic energies. Fig. 4a shows that the experimental fragment kinetic energy per nucleon is actually higher than the SMM

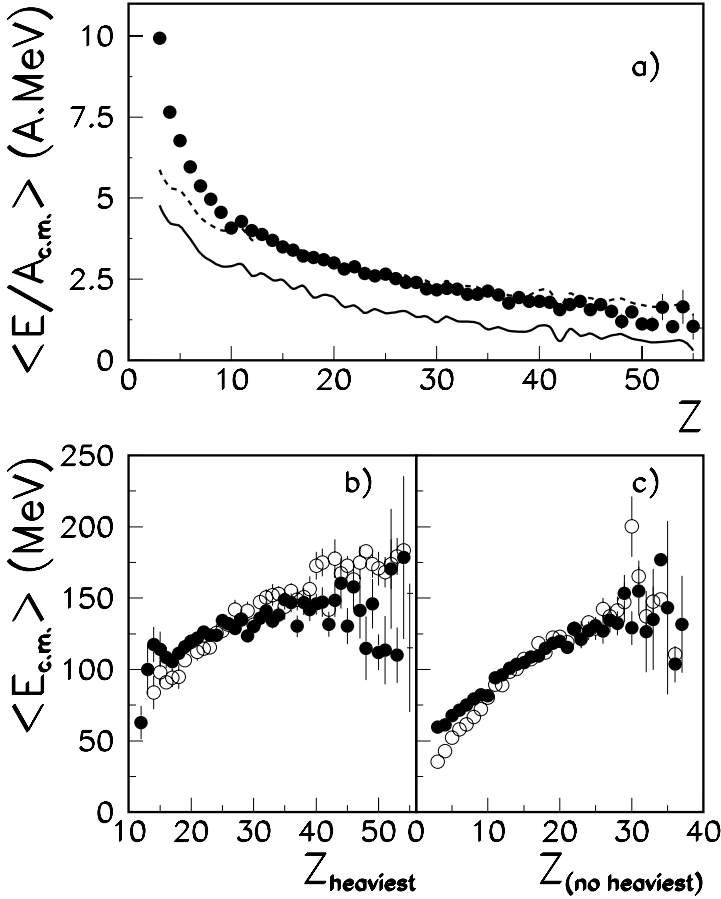


Fig. 4. Dynamic observables for the experimental sample (dots) and for the backtracing on SMM. (a) Mean c.m. kinetic energy per nucleon as a function of the fragment charge. The solid line is the SMM Coulomb+thermal fragment mean kinetic energy per nucleon, the dotted line corresponds to an addition of 1.1 A MeV. (b) Mean experimental (dots) and predicted (open circles) c.m. kinetic energy as a function of the fragment charge. Only the heaviest fragment in each event is considered. (c) Mean experimental and predicted c.m. kinetic energy for all fragments but the largest one. In panels (b) and (c) a mean collective energy 1.1 A MeV was added to the SMM Coulomb+thermal prediction.

prediction (full line). The resulting mean collective energy  $E_{\text{flow}}$  of 1.1 A MeV is in agreement with other measurements carried out in the same beam energy region. This result is close to the flow systematics threshold [6,12,36,37].

By adding this mean value to the mean predicted thermal+Coulomb energy (dashed line in Fig. 4a) a good reproduction of the mean experimental values is achieved, up to the maximum observed charge.

To detail the comparison further, we have separated the fragments into two classes, the first class containing the heaviest fragment in each event and the second one the remaining fragments. This procedure was suggested in Ref. [11] for a detailed study of the kinetic properties of the fragments. In both classes the centre of mass fragment kinetic

energies (Figs. 4b,c) are very well reproduced, indicating that the Coulomb energy was properly taken into account in the model by the freeze-out volume distribution obtained with the backtracing procedure. Volume fluctuations seem thus essential to reproduce the experimental dynamic observables.

The discrepancy observed in Figs. 4a,c for fragments with charge  $\leq 10$  can be explained by the fact that the simple addition of a constant collective energy can not take into account the geometry of light fragment emission. Indeed if these fragments are often emitted at the surface of the freeze-out volume, in average they will experience a larger collective energy.

This study should be completed by comparing the experimental and predicted energy standard deviations and energy spectra. To this aim the code should be run again by coupling the thermal and collective expansions. However, one has to remind that:

- From the data and model comparison an *average* value  $\approx 1.1$  A MeV of collective energy was deduced, but this does not imply the presence of a *constant* collective energy in the whole source space  $s$ .

The coupling between thermal and collective excitation energies can not be performed by simply adding a fixed amount of collective energy in the calculations. Theoretical prescriptions have to be followed.

The anticorrelation between the thermal excitation energy and the source volume seen in Fig. 1, the change of the amount of collective energy with the freeze-out volume found in Ref. [15] and the total energy conservation have to be taken into account to build a reasonable correlation between thermal and collective excitation energies.

- High (low) charge asymmetry experimental events (reproduced by SMM in small (larger) volumes) could correspond to a collective energy of different nature. For large volumes the collective energy could be radial flow, while for small volumes it could be rotational energy of the emitting system [8]. Following this picture the bulk of the events (corresponding to the most probable source volumes) could experience a mixing of rotation and flow [35].

From these considerations it follows that theoretical investigations are needed to identify the most sensitive observables to the different kinds of collective energy. Moreover a possible dynamical interpretation of the anticorrelation [ $E^{c.n.}$ ,  $V^{c.n.}$ ] requires more careful studies of dynamic observables. This relationship indeed could be viewed as due to the detection of events produced at different times of the source expansion stage. Sources undergoing multifragmentation at earlier times are more compact and excited than sources living for a longer time.

To confirm or exclude such an interpretation a study on fragment dynamic correlations is needed, but this study is beyond the aim of this paper.

## 7. Hidden observables

Hidden variables are the variables that cannot be evaluated either because they are substantially altered by the experimental filter or because they correspond to particles and fragments which cannot be disentangled from the others. The backtracing procedure can be used to determine these event characteristics depending on theoretical treatment. This is done by making the assumption that the features of the experimental and simulated events falling into the same square of the observable space (here the four dimensional principal space of Fig. 1a and Fig. 1b are the same). Thus a natural estimator of a variable which cannot be directly measured experimentally (*hidden* variable) is the weighted mean value of this variable for the simulated events. This estimator has a sampling distribution which is simply the distribution of the variable for the simulated events. Due to the properties of the mean value, it can be shown that the estimator is unbiased and its sampling variance is the variance of the simulated distribution. This technique has been used to determine event by event the multiplicities of pre-equilibrium protons and  $\alpha$  particles.

We can then firstly estimate the predicted multiplicities of protons and  $\alpha$  particles emitted by the composite nucleus and hot primary fragments ( $n_p^{c.n.}(\mathbf{p})$ , ( $n_\alpha^{c.n.}(\mathbf{p})$ ) in each square of the principal space  $\mathbf{p}$  in which fall the experimental events (Fig. 1 upper row). Hence, for an experimental event characterized by the principal vector  $\mathbf{p}$ , with  $n_p^{\text{det}}$  protons and  $n_\alpha^{\text{det}}$  alpha particles, the multiplicity of pre-equilibrium protons and  $\alpha$  particles can be respectively estimated by:

$$n_p^{\text{p.e.}} = \frac{n_p^{\text{det}}}{\langle \epsilon_p(\mathbf{p}) \rangle} - \langle n_p^{c.n.}(\mathbf{p}) \rangle, \quad (5)$$

$$n_\alpha^{\text{p.e.}} = \frac{n_\alpha^{\text{det}}}{\langle \epsilon_\alpha(\mathbf{p}) \rangle} - \langle n_\alpha^{c.n.}(\mathbf{p}) \rangle, \quad (6)$$

where  $\langle \epsilon_p(\mathbf{p}) \rangle$  and  $\langle \epsilon_\alpha(\mathbf{p}) \rangle$  are the event by event estimators of the detection efficiency for protons and  $\alpha$  particles.

The advantages of this method are that, on the one hand, we obtain information on an event by event basis and, on the other, the global experimental information is used to calculate the estimators. A result of this analysis is given in Fig. 5 which shows the correlation between the multiplicities of pre-equilibrium proton and  $\alpha$  particles. On average, the number of protons is twice the number of alpha particles with a broad distribution. The system can loose up to  $\sim 50\%$  of its constituents before the formation of the hot source.

Finally we point out that the evaluation of pre-equilibrium relies on three assumptions. The first one is that the agreement of the SMM events with the experimental events is also valid before the experimental filter, then that pre-equilibrium is composed of neutrons, protons and alpha particles (the method is obviously not sensitive enough to predict hydrogen and helium isotope yields [13,38] and heavier charges possibly produced in the pre-equilibrium stage) and, finally, that the detection efficiencies do

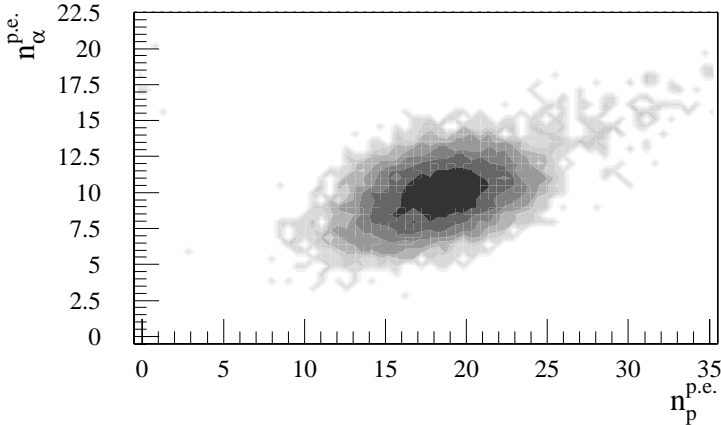


Fig. 5. Estimated correlation between the multiplicities of pre-equilibrium proton and  $\alpha$  particles.

not depend on the origin of light particles (as already mentioned, pre-equilibrium and equilibrium particles have similar mean emission velocities).

The pre-equilibrium protons and  $\alpha$ -particles multiplicities found through the backtracing method can be checked by a simple calculation based on the mean values of the detected observables. The mean total charge detected in form of fragments ( $Z \geq 3$ ) results  $\sim 92$ , the multiplicities of protons and  $\alpha$ -particles (obtained multiplying by two the multiplicity of the *isotropic* component, i.e. the number of protons and  $\alpha$ s emitted in the window of  $\theta_{c.m.}$  from  $60^\circ$  to  $120^\circ$  [11]) are  $\sim 13$  and  $\sim 7$  respectively. Thus a reasonable experimental estimate of the charge of the multifragmenting system is  $\sim 119$ . Charge conservation ( $\sim 39$  charges left for the pre-equilibrium) and the requirement that the *isotropic* light particle component and the pre-equilibrium one have the same mean charge  $\sim 1.37$ , lead to an evaluation of the pre-equilibrium multiplicities  $\sim 18$  and  $\sim 10$  for protons and  $\alpha$ -particles respectively, in agreement with the backtracing mean values.

From the previous analysis, it is possible to determine the mean  $Q$ -value corresponding to the formation of the hot source and the pre-equilibrium emission ( $-Q^{p.e.} = 0.77$  GeV). The mean velocities of pre-equilibrium particles are given by the backtraced simulation ( $E_{kin}^{p.e.} = 1$  GeV), so that the total pre-equilibrium energy is  $E^{p.e.} = 1.77$  GeV, which represents one half of the system energy. Furthermore, the averages of the  $Q$ -value and of the total kinetic energy corresponding to the composite nucleus have been evaluated for the events belonging to the bump (Fig. 1 upper row) making the assumption that these values are the same for the experimental sample and for the backtraced one ( $-Q^{c.n.} = 0.3$  GeV and  $E_{kin}^{c.n.} = 1$  GeV). The sum of these two figures is the mean thermal excitation energy of the composite nucleus ( $E^{c.n.} = 1.3$  GeV). Since the superimposed radial flow energy corresponds to 0.32 GeV, we obtain a total energy for the event of  $E_{tot} = 3.39$  GeV in agreement with the total available centre of mass energy  $E_{c.m.} = 3.45$  GeV.

## 8. Conclusions

In conclusion physical variables which cannot be directly measured were investigated by working in the framework of the statistical model SMM through an automatic backtracing procedure.

Sources variables ( $A^{c.n.}$ ,  $E^{c.n.}$ ,  $V^{c.n.}$ ), inputs of the simulation code, were treated as event by event parameters and provided informations on the freeze-out condition of the experimental events. The resulting scenario for our central collisions corresponds to the fragmentation of a very large and diluted composite system, just above the threshold of the flow development.

Due notably to the large spread of the number of pre-equilibrium particles the standard deviation of the break-up volume is large so that the distribution cannot be reduced to its mean value. Thus each observable distribution has to be calculated as a weighted sum of the distributions obtained for different values of the source variable  $s$ .

A mean collective energy of  $\sim 1.1$  A MeV results from the comparison between the charge by charge mean c.m. energies seen in the experiment and the calculated ones. This value is in agreement with other experiments performed at MSU [12], at GANIL with INDRA and NAUTILUS [6,36], and, for lighter nuclei, at ISN with AMPHORA [39,18].

Volume fluctuations are seen to be essential to reproduce the mean experimental dynamic observables. Further experimental and theoretical investigations on fragment dynamic correlations are needed, in order to properly introduce in the model the thermal and collective (radial flow or rotation) excitation energies on an event by event basis. A deeper investigation on the effects of collective energy on the dynamic observables should also allow to understand to which extent the break-up density distribution can be connected to the time evolution of the multifragmenting source.

## Acknowledgements

The authors would like to thank F. Gulminelli for many interesting, stimulating and constructive discussions.

This work has been supported in part by grants of the Italian Ministry of University and Scientific and Technological Research (MURST).

## References

- [1] Sa Ban-Hao and D.H.E. Gross, Nucl. Phys. A 437 (1985) 643;  
O. Shapiro and D.H.E. Gross, Nucl. Phys. A 573 (1994) 143; A 576 (1994) 428.
- [2] J.P. Bondorf, A.S. Botvina, A.S. Iljinov, I.N. Mishustin, K. Sneppen, Phys. Rep. 257 (1995) 133;  
A.S. Botvina et al., Nucl. Phys. A 475 (1987) 663.
- [3] W.A. Friedman, Phys. Rev. C 42 (1990) 667.
- [4] F. Gulminelli and D. Durand, Nucl. Phys. A 615 (1997) 117.
- [5] P. Danielewicz, Phys. Rev. C 51 (1995) 716.

- [6] M.F. Rivet et al., XXXV Int. Winter Meeting on Nuclear Physics, Bormio, February 1997, ed. I. Iori, Ric. Sc. and E.P. 110 (1997).
- [7] M. Colonna, Ph. Chomaz and A. Guarnera, Nucl. Phys. A 613 (1997) 165.
- [8] A.S. Botvina and D.H.E. Gross, Nucl. Phys. A 592 (1995) 257.
- [9] W. Reisdorf et al., Proc. Int. Workshop XXII, Hirshegg 1994, ed. H. Feldmeier and W. Nörenberg, p. 93;  
W. Reisdorf et al., Nucl. Phys. A 612 (1997) 493.
- [10] W.C. Hsi et al., Phys. Rev. Lett. 25 (1994) 3367;  
G.J. Kunde et al., Phys. Rev. Lett. 24 (1995) 38.
- [11] N. Marie et al., Phys. Lett. B 391 (1997) 15.
- [12] C. Williams et al., Phys. Rev. C 55 (1997) R2132.
- [13] R. Bougault et al., XXXV Int. Winter Meeting on Nuclear Physics, Bormio, February 1997, ed. I. Iori, Ric. Sc. and E.P. 110 (1997).
- [14] J.P. Bondorf, A.S. Botvina, I.N. Mishustin and S.R. Souza, Phys. Rev. Lett. 73 (1994) 628.
- [15] M. D'Agostino et al., Phys. Lett. B 371 (1996) 175.
- [16] P. Désesquelles, J.P. Bondorf, I.N. Mishustin and A.S. Botvina, Nucl. Phys. A 604 (1996) 183.
- [17] A.S. Botvina et al., Nucl. Phys. A 584 (1995) 737.
- [18] M. Charvet, Ph.D. Thesis, Univ. J. Fourier, Grenoble-I, France (1997).
- [19] P. Désesquelles et al., Phys. Rev. C 53 (1996) 2252.
- [20] R.T. DeSouza et al., Nucl. Instr. and Meth. A 295 (1990) 109.
- [21] I. Iori et al., Nucl. Instr. and Meth. A 325 (1993) 458;  
M. Bruno et al., Nucl. Instr. and Meth. A 311 (1992) 189;  
N. Colonna et al., Nucl. Instr. and Meth. A 321 (1992) 529;  
P.F. Mastinu et al., Nucl. Instr. and Meth. 338 (1994) 419.
- [22] V. Latora, M. Belkacem and A. Bonasera, Phys. Rev. Lett. 73 (1994) 1765;  
M. Belkacem, V. Latora and A. Bonasera, Phys. Rev. C 52 (1995) 271;  
M. Belkacem et al., Phys. Rev. C 54 (1996) 2435.
- [23] M. D'Agostino et al., Phys. Rev. Lett. 75 (1995) 4373.
- [24] M. D'Agostino et al., Phys. Lett. B 368 (1996) 259.
- [25] M.B. Tsang et al., Phys. Rev. Lett. 71 (1993) 1502.
- [26] M. D'Agostino et al., XXXIII Int. Winter Meeting on Nuclear Physics, Bormio, February 1995, ed. I. Iori, Ric. Sc. and E.P. 101 (1995).
- [27] J. Cugnon and D. L'Hote, Nucl. Phys. A 397 (1983) 519.
- [28] P. Désesquelles, Ann. Phys. Fr. 20 (1995) 1 (in English).
- [29] A.M. Kshirsagar, Multivariate Analysis (Marcel Dekker, Inc., New York, 1972).
- [30] E. Lloyd, Handbook of Applicable Mathematics, Vol. VI, Statistics, part B (Wiley, 1984).
- [31] R. Dennis Cook and S. Weisberg, Residuals and Influence in Regression, School of Statistics, University of Minnesota (Chapman and Hall, New-York, London, 1982).
- [32] B. Kämpfer et al., Phys. Rev. C 48 (1993) R955.
- [33] Bao-Han Li, A.R. DeAngelis and D.H.E. Gross, Phys. Lett. B 303 (1993) 225.
- [34] P. Kreuz et al. Nucl. Phys A 556 (1993) 672.
- [35] M. D'Agostino et al., XXXV Int. Winter Meeting on Nuclear Physics, Bormio, February 1997, ed. I. Iori, Ric. Sc. and E.P. 110 (1997).
- [36] R. Bougault, Nouvelles du GANIL, nr. 58, Caen (1996) 6.
- [37] B. Borderie, Proc. Int. Symp. on Large-Scale Collective Motion of Atomic Nuclei, Brolo (Messina) Italy, October 1996.
- [38] M.J. Huang, W.G. Lynch, H. Xi, M.B. Tsang, et al., MSUCL-1065, March 1997.
- [39] D. Heuer et al., Phys. Rev. C 50 (1994) 1943.